

Supplementary information

pH-Responsive Targeted Gold Nanoparticles for in vivo
Photoacoustic Imaging of Tumor Microenvironment

Shiyong Li ^{† b}, Kwok Ho Lui ^{† b}, Tik-Hung Tsoi^b, Wai-Sum Lo^b, Xin Li ^b, Xuesen Hu^b,
William Chi-Shing Tai^b, Clara Hiu-Ling HUNG ^c, Yan-Juan Gu^{*b}, Wing-Tak Wong ^{*a, b}

^a *The Hong Kong Polytechnic University Shenzhen Research Institute, Shenzhen, 518057, China.*

^b *Department of Applied Biology and Chemical Technology, The Hong Kong Polytechnic University, Hung Hom, Hong Kong, China. E-mail address: w.t.wong@polyu.edu.hk*

^c *University Research Facility in Life Science, The Hong Kong Polytechnic University, Hung Hom, Hong Kong, China.*

*Corresponding authors

Material and Methods

General

Dulbecco's Modified Eagle Medium (DMEM) and Minimum Essential Medium for cell growth was purchased from HyClone. Fetal bovine serum (FBS) and penicillin-streptomycin (PS) were obtained from GIBCO. Other reagents were obtained from Aldrich and used as received without further purification. Water was triply distilled using a Millipore filtration system. Solutions of HAuCl_4 and NaBH_4 were freshly prepared in distilled water, and all the reactions were conducted at room temperature (RT). UV/Vis absorption spectra were obtained using an Agilent 8453 UV-Vis spectrophotometer. Hydrodynamic size measured using a Malvern Zetasizer Nano S. Transmission electron microscope (TEM) images were recorded using a JEOL JEM-2100. PA images were acquired by a Vevo Sonic System consisting of Nd:Yag pump laser, tunable OPO, 21-MHz ultrasound transducer system. To match acoustic impedance, US gel was used.

Synthesis of 13-nm Gold Nanoparticles

Gold nanoparticles (AuNPs) with a 13 nm diameter were synthesized by reducing a well-stirred solution of 100 mL of 1 mM chloroauric acid with 10 mL of 38.8 mM sodium citrate in deionized water under reflux. The solution was stirred for several hours to allow full reduction. A red-wine-colored solution was cooled down to the room temperature. The particle concentration was estimated at ~ 14 nM, with an extinction coefficient of 5.6×10^8 at the peak of 520 nm with 1 cm path length. The solution was kept at 4 °C and in dark condition.

Cytotoxicity of the nanoprobe

Cell viability was measured using 3-(4,5-dimethylthiazol-2-yl)-2,5-diphenyltetrazolium bromide (MTT) proliferation assay. U87 MG cells were seeded at a cell density of 5×10^3 in a 96-well plate. After 24 h, the nanoprobe with different volume was added into each well with five duplications for each probe so as the concentration to reach 5, 10, 20, 40 and 80 nM. The cell culture medium was set as control. The cell viability after exposure to nanoprobe was compared to that of the blank control. The treatment medium was removed after 24 hrs of co-incubation and the cells were washed three times with 1x PBS. Then, 100 μl of the MTT solutions (0.5 mg/ml in PBS) was added to each well. After 4 h of co-incubation, the MTT medium was removed and formazan crystals were dissolved with 100 μl DMSO/EtOH mixture (1:1), and the solution was vigorously mixed to dissolve the reacted dye. The absorbance was measured at 490 nm on a Spectra Max[®] M3 Microplate Reader.

Real-time PCR of U87 MG tumor

All the test reagents including Trizol Reagent (CW0580S, CWBIO) Ultrapure RNA (CW0581M, CWBIO) HiFiScript cDNA (CW2569M, CWBIO) and UltraSYBR Mixture (CW0957M, CWBIO). PCR products were analyzed by CFX Connect™ Real-Time PCR Detection System. The total RNA was isolated from U87MG tumor ($\alpha_v\beta_3$ integrin-positive) and MCF7 cells ($\alpha_v\beta_3$ integrin-negative) using Trizol reagent according to manufacturer's instruction, and then reverse transcribed with a mixture of random hexamer primer, 5 \times room-temperature buffer, DTT, and 50U of M-MLV reverse transcriptase. The sequences of the forward and reverse primers of α_v were 5'-GAAAAGAATGACACGGTTGC and 5'-TAACCAATGTGGAGTTGGTG, respectively. The sequences of the forward and reverse primers of β_3 were 5'-ACTGCCTGTGACTC-CGACT and 5'-GGCTCTGGT GAGCAAGAAACA. The sequences of the forward and reverse primers of β -actin were 5'-ACCAGGGCTGCTTT-TAACTCT and 5'-GAGTCCTCCACGATACCAAA. The PCR reaction (95 °C for 15s, 57.5 °C for 60 s, 95 °C for 15 s, 57.5 °C for 15 s) was run for 30 cycles after

an initial single cycle of 95 ° C for 5 min to activate the Taq polymerase. The result was analyzed by the 2- $\Delta\Delta$ CT method that has been extensively used as a relative quantification strategy for quantitative real-time polymerase chain reaction (qPCR).

The LC/MS Instrument: Agilent 1290 UHPLC/Agilent 6540 ESI-QTOF-MS

Mobile phase A: H₂O, 0.1% formic acid, Mobile phase B: ACN, 0.1% formic acid, Gradient: 13 min linear gradient from 5% B to 90% B., Flow rate: 0.3 ml/min, Column: Agilent EclipsePlus C18 (2.1 x 50 mm, 1.8 μ M)

ESI: Positive mode

Synthesis of the Crocoines dye

2,3,3-trimethylindoleine (318 mg, 2 mmol) and croconic acid (145 mg, 1 mmol) were heated at reflux in a mixture of 10 ml butanol and 10 ml benzene; the water was removed azeotropically using Dean-Stark trap. The reaction was monitored by UV-vis/NIR spectroscopy until the complete disappearance of precursor bands. The reaction mixture was kept overnight at -20 °C. The crystals were filter out with cool ether. Further recrystallization with methanol gave a high purity compound. Yield 322 mg (75%).

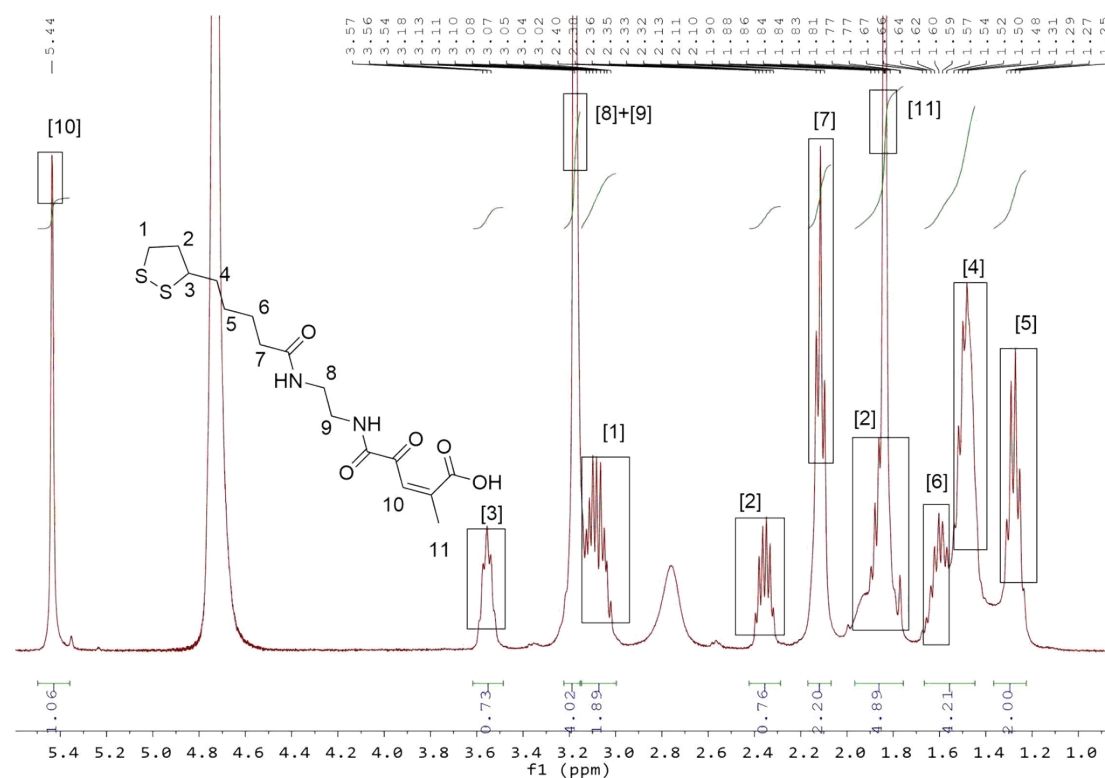


Fig. S1 ¹H NMR spectrum of 4-(2-(5-(1,2-dithiolan-3-yl)pentanamido)ethylamino)-2-methyl-4-oxobut-2-enoic acid(LSC) ligand in D₂O.

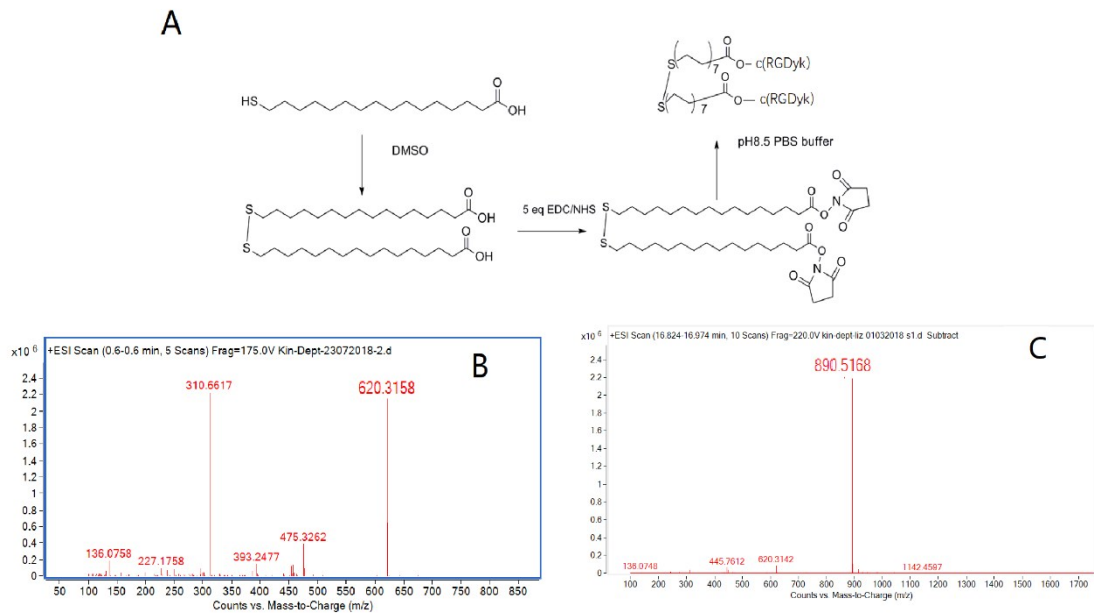


Fig. S2 Schematic of preparation c(RGDyK)-MHDA ligand (A) The UPLC-MS spectra of prepared c(RGDyK)-MHDA (C) and cyclic c(RGDyK) (B).

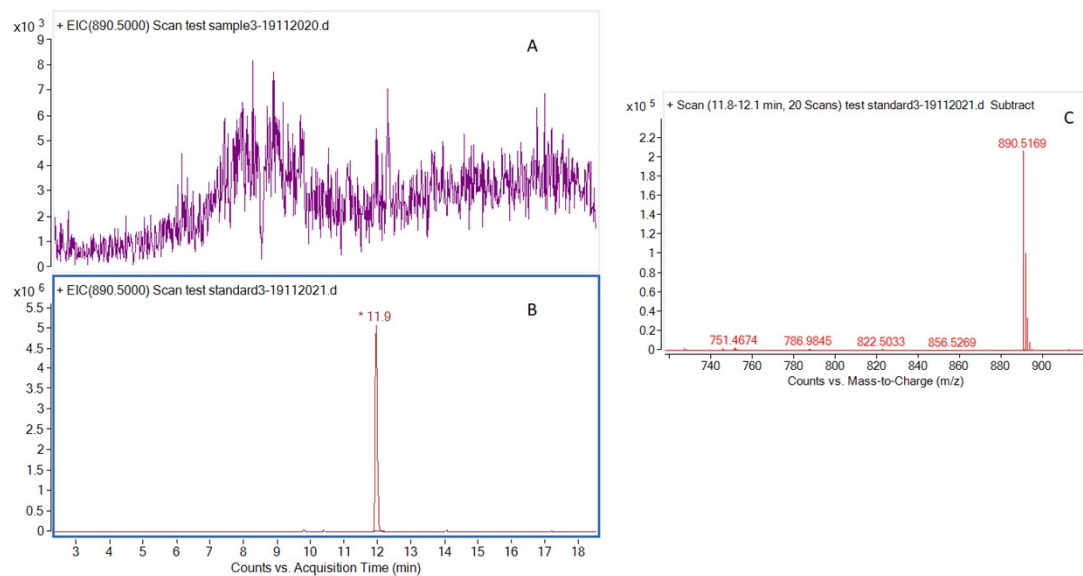


Fig. S3 (A) LC chromatograph of the c(RGDyk)-MHDA/LSC in filtrate after wash with ultrafiltration, (B) LC chromatography of the c(RGDyk)-MHDA/LSC molecules for conjugation, (C) UPLC-MS spectra of prepared c(RGDyk)-MHDA.

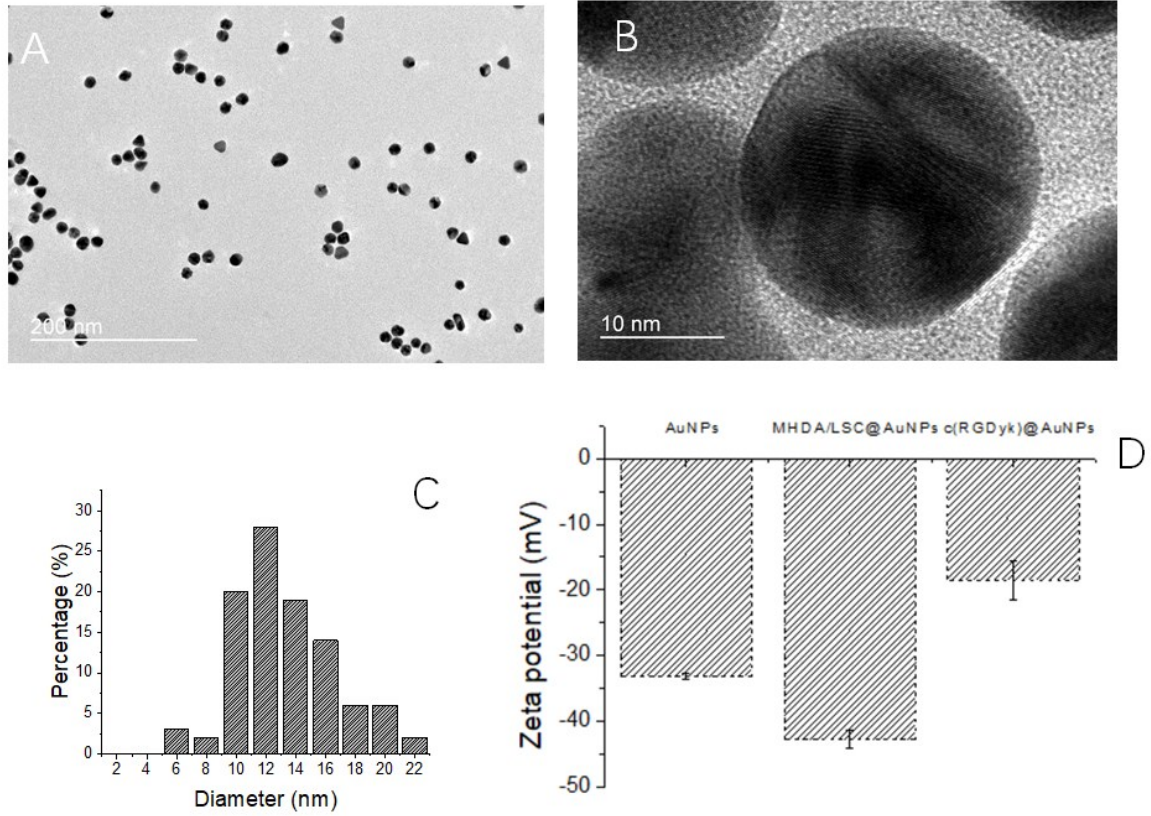


Fig. S4 (A) TEM image of citrate-capped AuNPs. (B) High resolution TEM image of AuNPs. (C) The average size of AuNPs is around 12.2 ± 1.1 nm. (D) The Zeta Potential of citrate-capped AuNPs, MHDA/LSC@AuNPs and c(RGDyk)-MHDA/LSC@AuNPs.

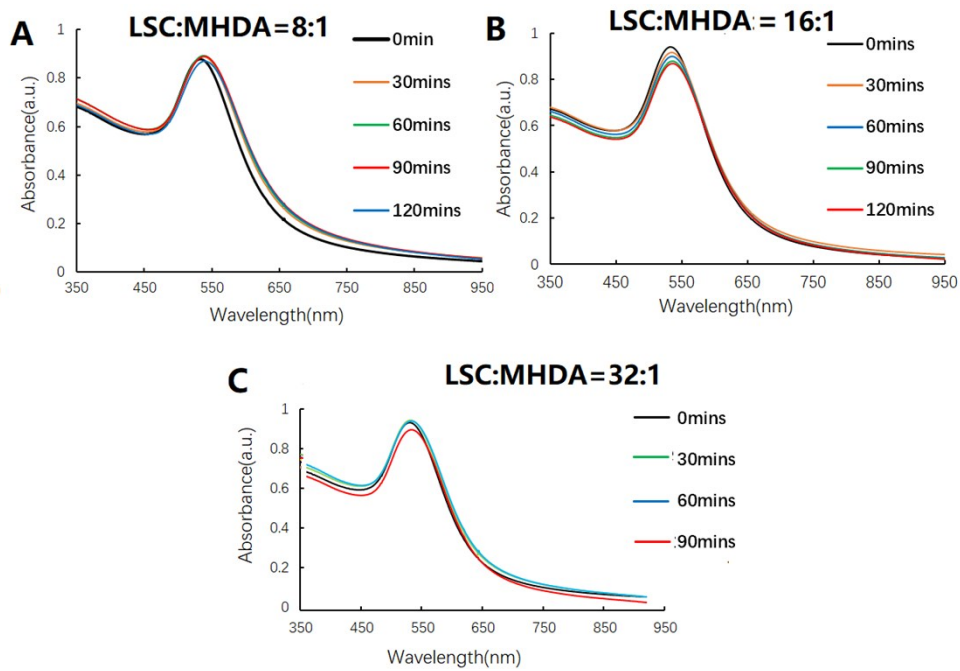


Fig. S5 (A-C) Time evolution of absorption spectra of c(RGDyk)-MHDA/LSC@AuNPs at pH 5.8. When the feeding ratio of LSC to MHDA ligands ranges larger than 32:1, the modified nanoparticles exhibited stable at pH 5.8 buffer solution even after 2 hrs incubation.

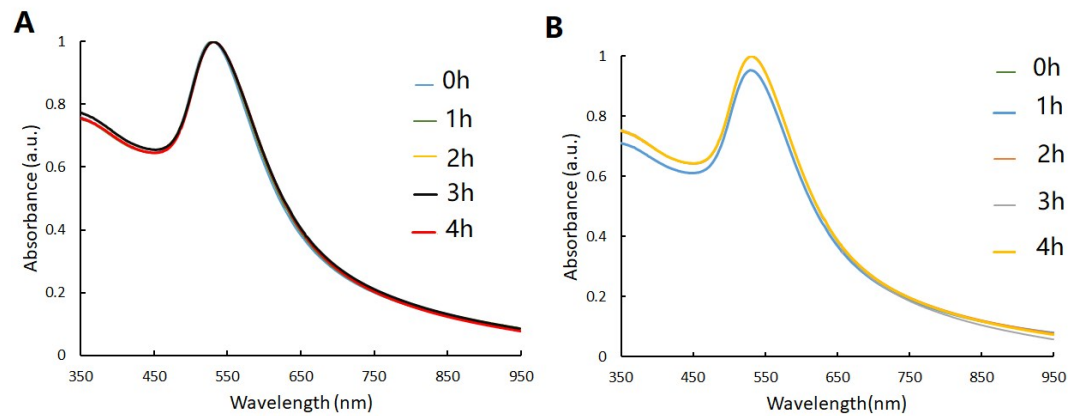


Fig. S6 Stability of MHDA/LSC@AuNPs in 10 mM PB buffer at pH 5.8 (A) and pH 7.4 (B).

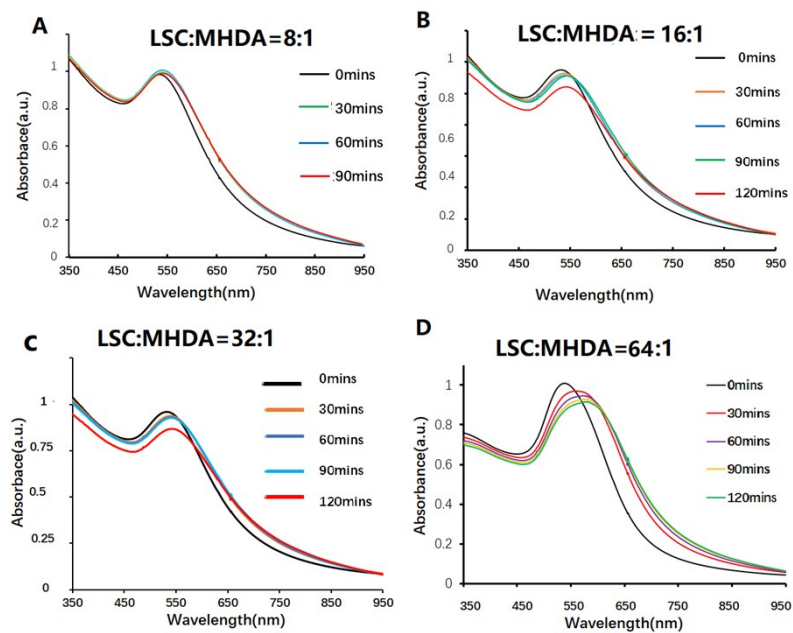


Fig. S7 (A-D) Time evolution of absorption spectra of c(RGDyk)-MHDA/LSC@AuNPs at pH 6.5. When the feeding ratio of LSC to MHDA ligands ranges larger than 32:1, the modified nanoparticles exhibited stable at pH 5.8 buffer solution even after 2 hrs incubation.

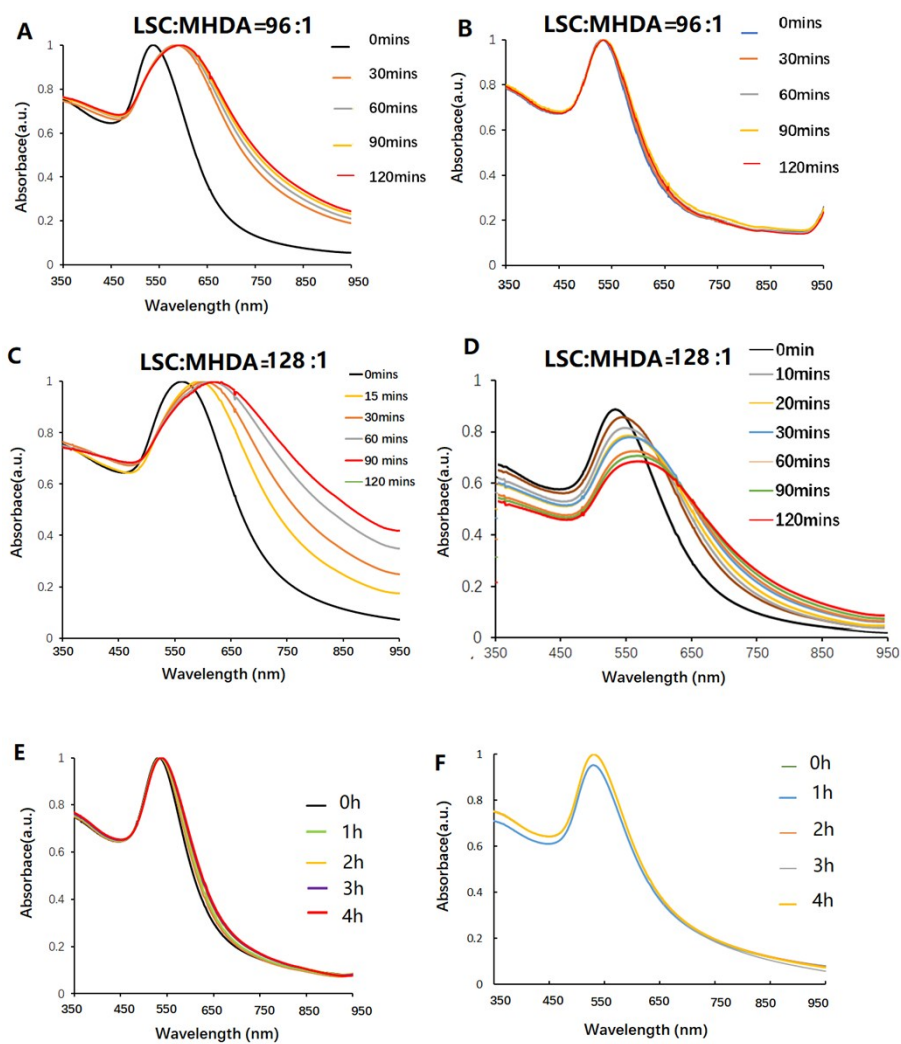


Fig. S8 (A to D) Time evolution of absorption spectra of c(RGDyk)-MHDA/LSC@AuNPs at pH 6.5(A and C) and pH7.4(B and D). When the feeding ratio of LSC to MHDA ligands ranges larger than 96:1, the modified nanoparticles exhibited red-shifted to NIR range. (E and F) Stability of MHDA/LSC@AuNPs in 10 mM PB buffer at pH 6.5 (A) and pH 7.4 (B).

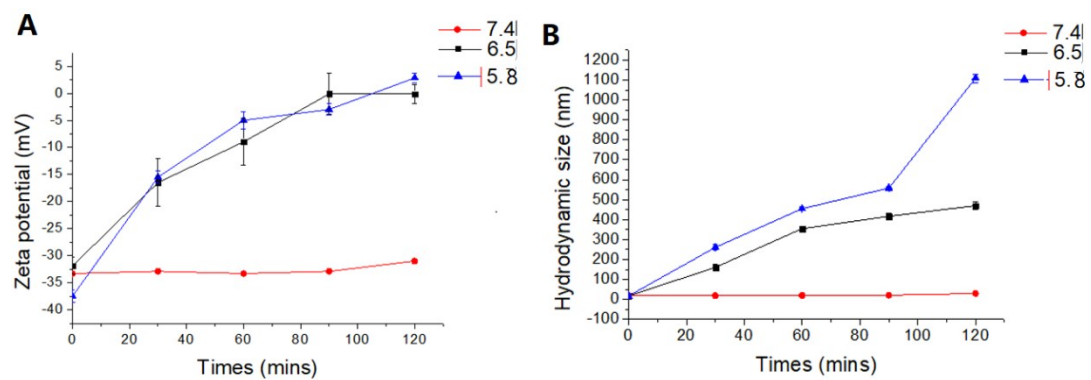


Fig. S9 Time evaluation of zeta potential (A) and DLS (B) measurement of MHDA/LSC@AuNPs in pH 7.4, 6.5 and pH5.8 phosphate buffer (10 mM) at different time points.

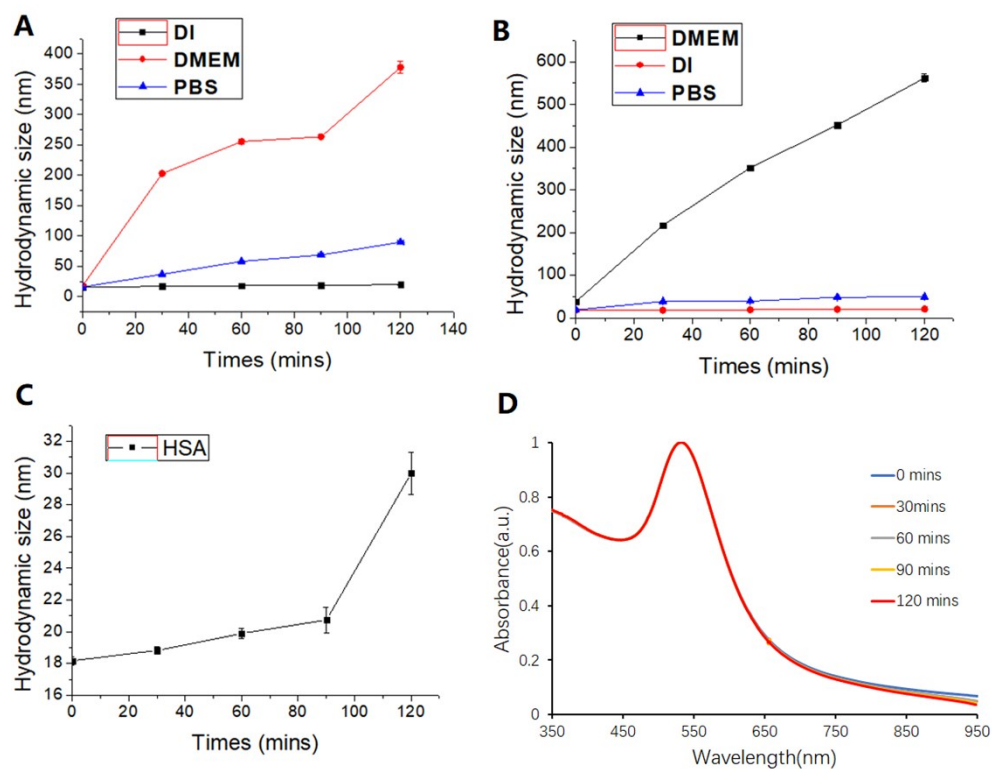


Fig. S10 (A) DLS measurement of c(RGDyk)-MHDA/LSC@AuNPs in PBS (pH 7.4), DMEM and DI water at different time point. (B) DLS measurement of MHDA/LSC@AuNPs in PBS (pH 7.4), DMEM and DI water at different time point. (C) DLS measurement of c(RGDyk)-MHDA/LSC@AuNPs in HSA solution. (D) Time evolution of absorption spectra of c(RGDyk)-MHDA/LSC@AuNPs at (35 mg/ml) HSA.

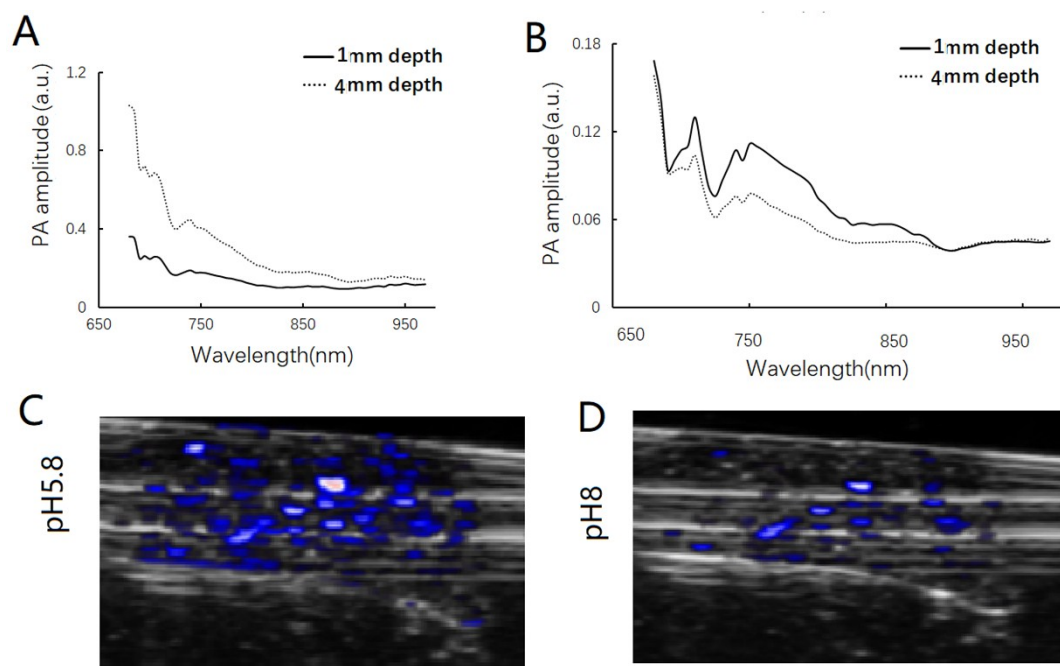


Fig. S11 Photoacoustic activities of nanoparticles. Photoacoustic activity-wavelength profiles of the targeted nanoprobe in pH 6.5 (A) and pH 8 (B) phosphate buffer (C and D) in tissue-mimic phantom.

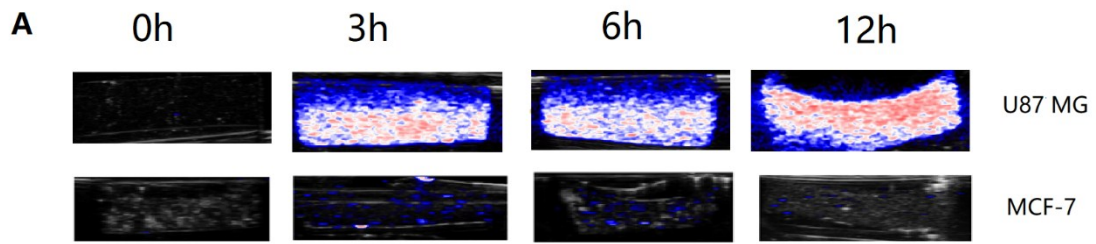


Fig. S12 Photoacoustic activities of nanoparticles. Photoacoustic activity-wavelength profiles of the targeted nanoprobe in tissue mimic phantom merged with U87MG and MCF-7 cell lines.

To evaluate the cytotoxicity of the c(RGDyk)-MHDA/LSC@AuNPs, we assessed cell proliferation by (3-(4,5-dimethylthiazol-2-yl)-2,5-diphenyltetrazolium bromide (MTT) assay (Fig. S12). The results proved that the targeted nanoprobe exhibited no obvious cytotoxicity under all test concentration after 24 hrs incubation. However, they exhibited moderate toxicity when the concentration up to 7.2 nM with a prolonged incubation time of 48 hrs in U87MG cell line.

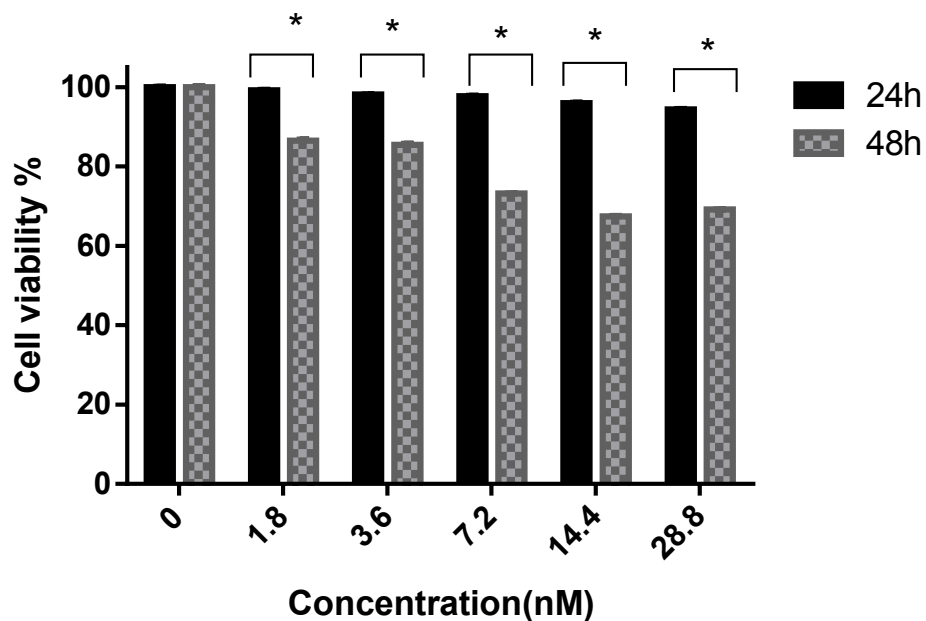


Fig. S13 Viability of U87MG cancer cells incubated with different concentrations of c(RGDyk)-MHDA/LSC@Au for 24 and 48 hrs. Error bars represent standard deviation (n = 5). *p<0.05.

The PCR data indicated a significant number of fragments being detected from the expression of α_v mRNA and β_3 mRNA in U87MG tumor while small amount of α_v or β_3 mRNA fragments were found from MCF7 cells (Fig. S14).

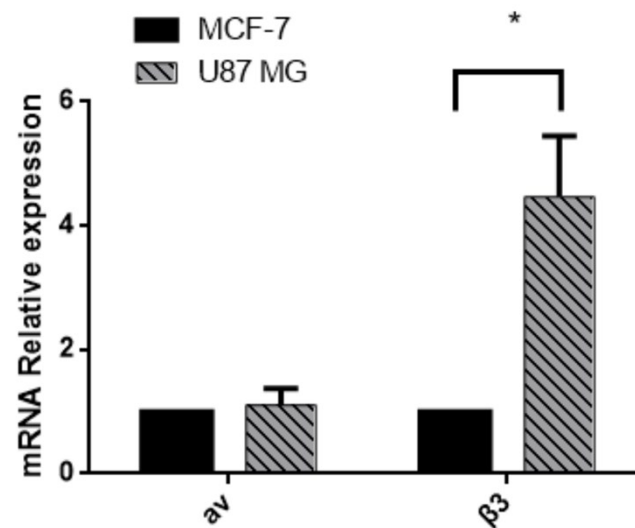


Fig. S14 RT-PCR analysis. Expressions of $\alpha_v\beta_3$ in U87MG tumor and MCF7 cells were determined by RT-PCR. Error bars represent standard deviation. * $p < 0.05$

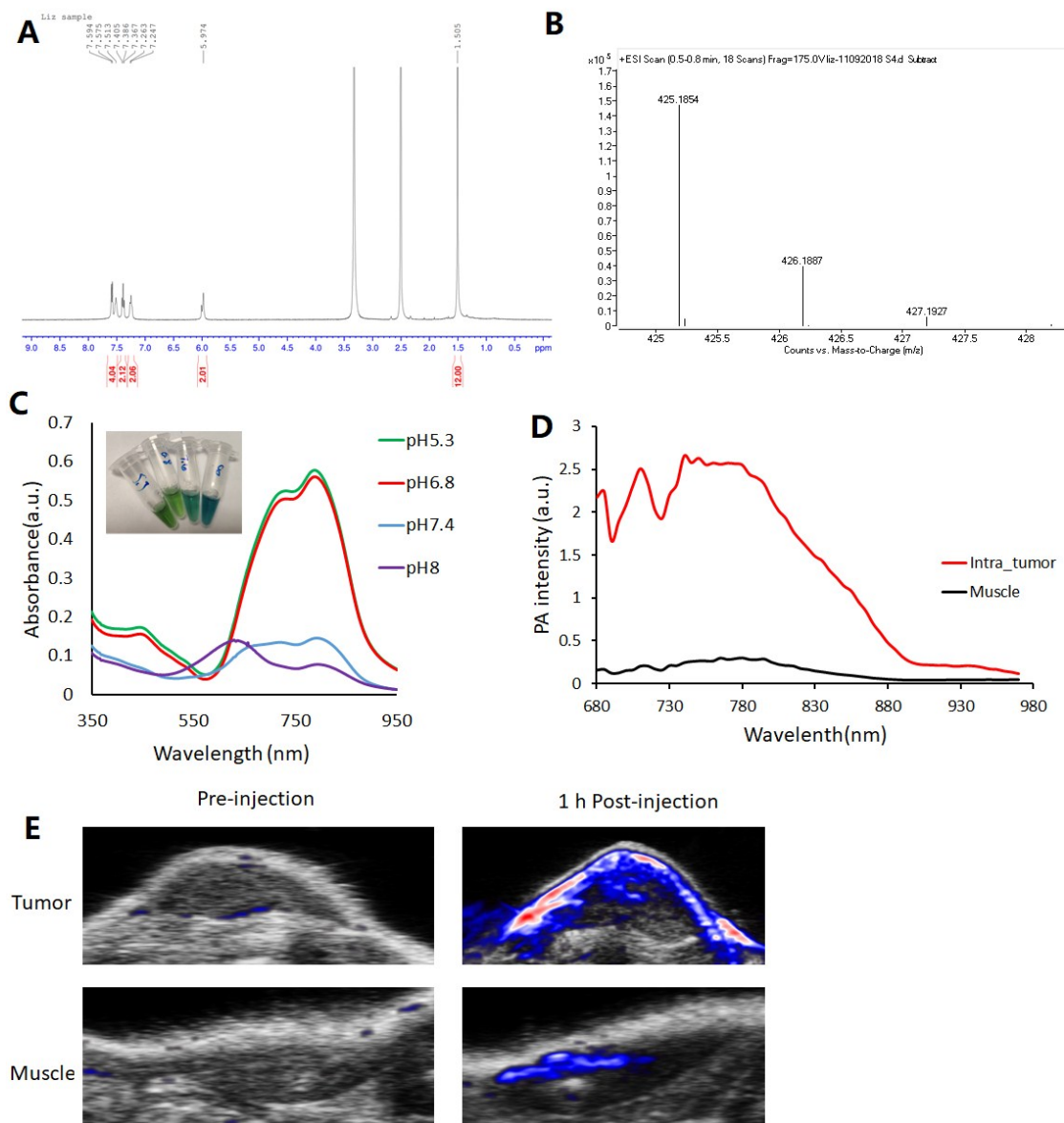


Fig. S15 (A) ¹H NMR spectrum of Croc in DMSO (B) The UPLC-MS spectra of prepared Croc. (C) UV-Vis-NIR absorbance spectra of Croc dispersed in buffers with different pH values with images. (D) Quantitative measurement of *in vivo* Croc PA spectra under tumor and normal muscle with the same volume injection of Croc. (E) PA imaging of Croc dispersed in tumor and normal muscle.

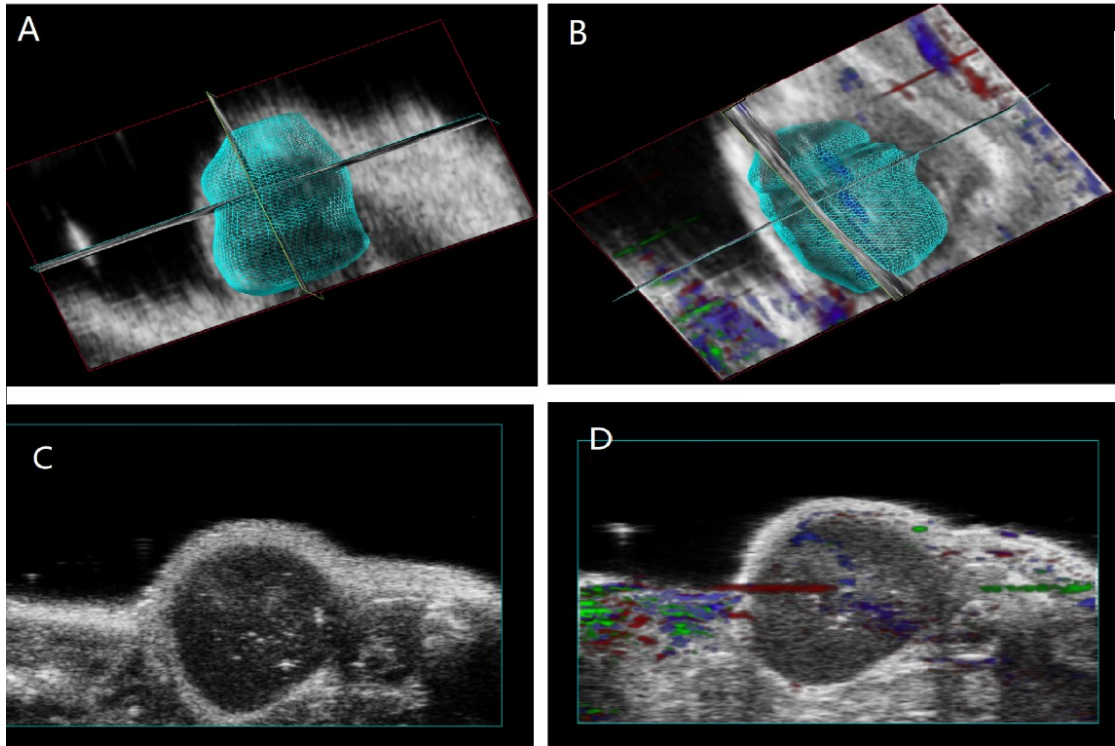


Fig. S16 In vivo PA imaging of subcutaneous tumors of U87 MG cells in mice. The perspective views of 3D volume rendering of PA images shown in pre-injection (A) and 24 hr post-injection (B) in which the oxygenated hemoglobin is shown in red and deoxygenated hemoglobin in blue and the spatial distribution of c(RGDyk)-MHDA/LSC@AuNPs in green. (C) and (D) as indicated one of the cross sections of the 3D tumor for the pre-injection and 24h post-injection. The pre-injection and post-injection volume size of tumor is 207.127 mm^3 and 225.647 mm^3 , which indicated no obvious toxicity.

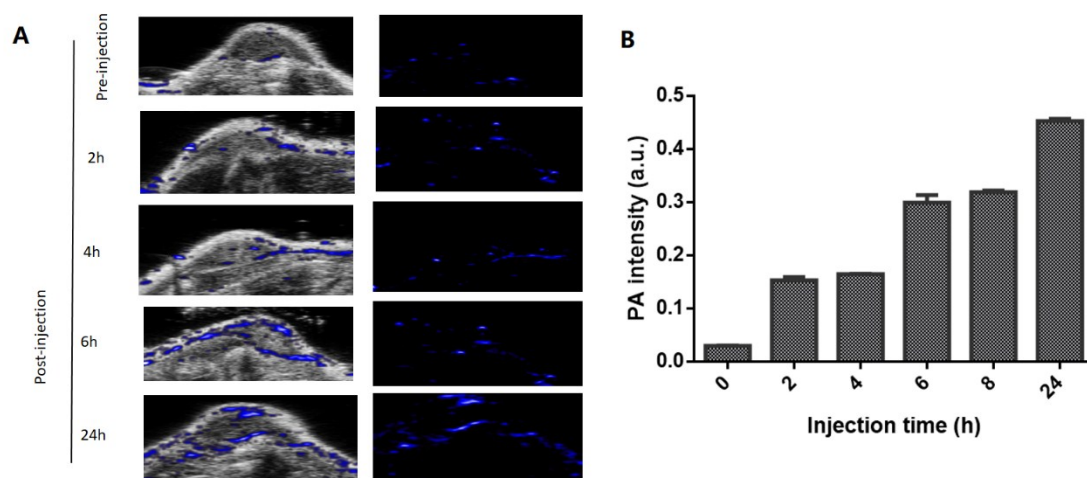


Fig. S17 Targeting of integrin $\alpha\beta3$ -positive U87MG tumors in mice by non-targeted nanoprobe. (A) Photoacoustic images and ultrasound images of nude mice bearing U87MG tumors were obtained before injection or at 2, 4, 6, and 24 hrs after intravenous injection of non-targeted nanoprobe MHDA@AuNPs (B) Average PA intensity increment at 680 nm as a function post-injection time of MHDA@AuNPs (n =2).